Rapid cell turnover to model adipocyte size distribution

Louis Fostier, Aloïs Dauger, Romain Yvinec, Magali Ribot, Chloe Audebert, Hédi Soula

Rapid cell turnover to model adipocyte size distribution

Louis Fostier[1,2], Aloïs Dauger[3,4], Romain Yvinec[1,2], Magali Ribot[6,7], Chloe Audebert[2,4,5,*], Hedi Soula[3]

[1] PRC, INRAE, Paris-Saclay, Université de Tours, 37380 Nouzilly, France
[2] Université Paris-Saclay, Inria, Centre Inria de Saclay, 91120 Palaiseau, France
[3] Sorbonne Université, Inserm, Nutrition and obesities: systemic approaches, Nutriomics, F-75013 Paris, France
[4] Sorbonne Université, Université Paris Cité, CNRS, Laboratoire Jacques-Louis Lions, LJLL, F-75005 Paris, France
[5] Sorbonne Université, CNRS, Laboratoire de Biologie Computationelle, Quantitative et Synthétique, CQSB, F-75005 Paris, France
[6] Institut Denis Poisson, Université d'Orléans, CNRS, Université de Tours, 45067 Orléans, France
[7] Université Paris-Saclay,MaIAGE, INRAE, 78350 Jouy-en-Josas, France
* chloe.audebert@sorbonne-universite.fr

Abstract

White adipose tissue, composed of adipocyte cells, primarily stores energy as lipid droplets. The size of adipocytes varies significantly within the tissue due to the amount of stored lipids, and their size distribution is uniquely bimodal, lacking a characteristic size. Previous modeling efforts to understand these characteristics fall into two categories. On the one hand, models that aim at replicating bimodality using general parameters: their broad nature makes it hard to associate with physiological mechanisms. On the other hand, mechanistic models are usually based on lipid exchanges and neglect cell renewal assuming adipocyte turnover is low.

We propose a novel dynamical model, based on a partial differential equation, where adipocytes are constantly growing in size, and when growth is slowed for a certain size, cells tend to accumulate at this size. In addition, it includes a recruitment and a death rate accounting for turnover. This model admits a unique stationary solution, locally asymptotically stable, for a wide choice of problem functions. The

stationary solution is parameterized with 3 parameters, that are uniquely estimated with measured cell size distributions. This explicit function gives a new way to fit adipocyte size distributions with only three parameters, which is a novel approach and gives results in good agreement with available data.
keywords: partial differential equation modeling, adipocyte size distribution, white adipocyte tissue, parameter estimation, stationary solution

1 Introduction

The global public health challenge posed by obesity has drawn significant interest from the scientific community. Defined as an excessive accumulation of white adipose tissue, obesity is associated with an increased risk of comorbidities such as type 2 diabetes, cardiovascular diseases, and certain cancers [23]. These obesity-related diseases are the consequences of white adipose tissue dysfunctions. A chronic energy imbalance results in lipid accretion in cells dedicated to storage: the adipocytes. This accumulation is enabled by two mechanisms: increasing the adipocyte number (hyperplasia) and increasing the adipocyte size (hypertrophy). In fact, adipocytes exhibit singular size properties with radii ranging from $7\,\mu$m to $150\,\mu$m and displaying a bimodal distribution with a peak around $10-12\,\mu$m and a second one around $50-60\,\mu$m [27]

An abnormal size of those cells may be the onset of a complete tissue impairment as it correlates with drastic physiological changes. First, at the cell scale: lipolysis, lipogenesis activity, adrenoceptor expression, insulin sensitivity, senescence are altered [13, 20, 27, 41]. Then, at the tissue scale through permanent crosstalk and interactions with the stroma-vascular fraction: macrophage infiltration, reduced angiogenesis, hypoxia and fibrosis [39, 40]. Finally, alterations are observed at a systemic scale: low-grade inflammation, glucose metabolism impairment, altered adipokine secretion and liver steatosis [32, 27, 22, 24, 33]. Thus, the size and number of adipocytes are key parameters in obesity. Whether they are drivers leading to the pathological state or indicators of it is not yet clear. However, it makes consensus that they play a pivotal role in the emergence and persistence of obesity.

In order to better understand these dynamics, few mathematical models have tried to address the issue of adipocyte size. In [17, 16, 18], the authors have proposed models based on partial differential equation to adipocyte size distributions in rats under various dietary conditions. They have assumed cell turnover and a size-dependent rate described by an imposed function where the associated parameters are difficult to relate to physiological processes. The adipocyte modeling in [25] is based

on three compartments and has been developed to describe small, medium and large adipocytes. The cell size evolution depends on lipid fluxes that are related to protein concentration controlling lipotoxicity – a cellular dysfunction due to lipid accumulation in non-adipose tissue. All these models provide studies of the adipose tissue growth dynamic and its bimodality through cell hyperplasia and/or hypertrophy, but the mechanisms governing lipid fluxes involved in adipocyte hypertrophy have not been considered and the models rely on large numbers of general parameters. More recently, authors in [1] have proposed a statistical approach to extract characteristics of cell size distribution for several participants before and after caloric restriction.

We previously have proposed mechanistic models based on lipid fluxes [36, 35, 9, 28, 6]. These models share common assumptions: a) there is only one adipocyte population type, b) cell's size is determined by lipid fluxes, c) the inflow and outflow are proportional to the surface area of the cell, d) cells do not experience apoptosis and no recruitment is accounted for, therefore the number of cells is constant. They differ on assumptions regarding the size differences between cells: in [9] and [28], we have considered partial differential equation models where a diffusion term is used to mimic cell population heterogeneity, whereas in [36] and [6] models are based on ordinary differential equations and intrinsic differences between cells are considered (by distributing some parameters over the cell population). The previous models do not take into account cell renewal (recruitment and death) and they strongly rely on a slow turnover of adipocytes (in humans 10% of fat cells are renewed annually [37]). However, it has been reported that 0.6% to 1.5% adipocytes are replaced each day for lean mice ad libitum [30, 29, 19]. It leads to re-evaluate the hypothesis of slow turnover of adipocyte cells in rats (the measurements considered previously and in this paper are measured in rats).

In this work, we propose a new mathematical model, based on a partial differential equation, that aims at modeling adipocyte size distributions taking into account cell turnover (cell "death" and "recruitment"). Adipocytes are "recruited" at a constant rate, with a common minimal radius. Cell size over time is related to lipid uptake assuming outflow of lipids can be neglected. Based on previous mechanical considerations, the magnitude of the uptake depends on the amount of extracellular lipids and on the radius on the cell, linking the growth rate to the lipid influx. More precisely this growth rate will be slow for small cells - since lipid influx depends on size - and is decreased for high radius due to tissue constraints. Since the growth rate is variable, cell will accumulate for size where the cells grow slowly. Assuming a constant death term prevents cells from accumulating at higher size. These properties allow us to obtain bimodal cell size distribution. The modeling assumptions and equations are described in section 2.1. The stationary solution is introduced in section 2.2. We show that this model admits a unique stationary solution, locally asymptotically stable (section 3.1). Numerical simulations are performed to explore the model output

sensitivity to parameters (section 3.2). Next, with adipocyte size distributions measured in rats, the model parameters are estimated (section 3.3), showing that the measurements are well reproduced (with only 3 parameters to estimate). Finally we conclude this paper with a discussion in section 4.

2 Model and Methods

2.1 Model for adipocyte size distribution

We present a new model of dynamics of adipocytes' size. It assumes that adipocytes are "recruited" at a constant rate ρ (cell.time^{-1}) and submitted to apoptosis at rate σ (time^{-1}), independent of age or size. Whenever a new adipocyte enters the population, it has a radius of r_{min} (μm) and incorporates lipids (and thus grows in size) at a speed that depends on its radius r and on the amount of extracellular lipid L (nmol). We assume that the growth speed has a separable form, defined as:

$$V(r, L) = f(L)g(r),$$

with f an increasing function of the extracellular lipid L, and g a positive continuous function of radius. This means that lipid availability and cell size influence lipid uptake independently and in a multiplicative manner, see Theorem 3 for more precise assumptions and Eq. (11) for a concrete modeling choice for parameter estimation. The extracellular amount term L is assumed to be pumped from the medium. The redistribution of lipids happens when a cell goes into apoptosis. It releases its lipid content in the medium and the cell is taken out from the pool.

We obtain a flow equation, that describes the evolution of the cell density $u(t, r)$ at time $t \in \mathbb{R}^+$ with radius $r \in [r_{min}; +\infty[$:

$$\frac{\partial}{\partial t}u(t, r) + \frac{\partial}{\partial r}\left(V(r, L(t))u(t, r)\right) = -\sigma u(t, r) \tag{1}$$

with boundary condition on $r = r_{min}$,

$$V(r_{min}, L(t))u(t, r_{min}) = \rho. \tag{2}$$

The extracellular (available) lipid quantity L depends on time t: it is increased whenever a cell dies and decreased when cells grow. The decrease depends on the amount of variation of the lipid content of a cell, denoted by $l(r)$ a function of cell radius r. The assumption that lipids are redistributed when cells exit the system leads to a conservation equation of total lipids. Therefore the content of lipids inside all cells (intracellular) $L_{\text{int}}(t)$ at time t being

$$L_{\text{int}}(t) := \int_{r_{min}}^{\infty} l(s)u(t, s)\mathrm{d}s\,, \tag{3}$$

we obtain that the total amount of lipids, L_0 (nmol), is constant at all times t:

$$L(t) + L_{\text{int}}(t) = L_0 \text{ for all } t \geq 0. \tag{4}$$

Differentiating in time, we obtain in particular that,

$$\begin{aligned}\frac{d}{dt}L(t) &= -\int_{r_{min}}^{\infty} V(s, L(t))l'(s)u(t,s)ds + \sigma \int_{r_{min}}^{\infty} l(s)u(t,s)ds \\ &= -f(L(t)) \int_{r_{min}}^{\infty} g(s)l'(s)u(t,s)ds - \sigma L(t) + \sigma L_0 \,.\end{aligned}$$

Equations (1), (2) and (4) with initial distribution $u(0,r) = u_0(r)$ for all $r \geq 0$ define a time-dependent size density function. Using fixed point argument on the function $t \mapsto L(t)$, one can show that global existence, uniqueness and non-negativity of solution $u \in \mathrm{L}^1\left((r_{min}, +\infty), (1 + l(x))\mathrm{d}x\right)$ holds under fairly general assumption, see e.g. [21, 5, 2].

We now give some explicit forms for the function l, f and g. Assuming spherical shape for the adipocytes, we can link l and r as:

$$V_l\, l(r) = \frac{4\pi}{3}r^3 - \frac{4\pi}{3}r_{min}^3, \tag{5}$$

where V_l (μm^3.nmol^{-1}) is a conversion constant [36]. An adipocyte captures lipids at a rate proportional to its surface area and cannot grow indefinitely, so the growth speed decreases with the radius when the radius becomes large, hence we can choose

$$g(r) = \frac{r^2}{1 + r^k\theta^{-k}}\,, \tag{6}$$

for some saturating constant $\theta > 0$ (μm) and exponent $k \geq 2$. Compared to the previous model introduced in [36], the growth speed is always strictly positive. In line with the previous model, adipocyte growth is proportional (via parameter $\alpha(\mu\text{m}^{-1}.\text{time}^{-1})$) to a sublinear (michaelian) input of extracellular lipid L with constant κ (nmol), defined as:

$$f(L) = \alpha\frac{L}{L + \kappa}\,. \tag{7}$$

2.2 Stationary solution

This new model assumes only lipogenic activity. Compared with the previous model we have considered [36], there is no equilibrium between lipogenesis and lipolysis. We can still derive a stationary distribution and a cell number evolution.

Let's call $N(t)$ the total number of cells at time t defined as:

$$N(t) = \int_{r_{min}}^{\infty} u(t,s)\mathrm{d}s.$$

By integrating Eq.(1) over r we obtain:

$$\int_{r_{min}}^{\infty} \frac{\partial}{\partial t} u(t,s)\mathrm{d}s + \int_{r_{min}}^{\infty} \frac{\partial}{\partial r} \left(V(s,L(t))u(t,s)\right)\mathrm{d}s = -\sigma \int_{r_{min}}^{\infty} u(t,s)\mathrm{d}s$$

then

$$\frac{d}{dt}\int_{r_{min}}^{\infty} u(t,s)\mathrm{d}s - V(r_{min},L(t))u(t,r_{min}) = -\sigma \int_{r_{min}}^{\infty} u(t,s)\mathrm{d}s$$

which leads to

$$\frac{dN}{dt}(t) - \rho = -\sigma N(t).$$

From this equation, we derive the number of cells at equilibrium

$$N^\star = \frac{\rho}{\sigma}$$

and calling $u^\star$ a stationary solution of Eq. (1), it satisfies the following equation:

$$\frac{d}{dr}\left(V(r,L^\star)u^\star(r)\right) = -\sigma u^\star(r),$$

where $L^\star$ is the stationary number of extracellular lipids satisfying conservation equation (4). Then, since $V(r,L^\star) > 0$ when $r \geq r_{min}$,

$$\frac{d}{dr}\left(V(r,L^\star)u^\star(r)\right) = -\frac{\sigma}{V(r,L^\star)} V(r,L^\star)u^\star(r)$$

and then

$$V(r,L^\star)u^\star(r) = \rho \exp\left(-\int_{r_{min}}^{r} \frac{\sigma}{V(s,L^\star)}\mathrm{d}s\right)$$

with $V(r_{min},L^\star)u^\star(r_{min}) = \rho$.

For the sake of clarity, we now add a dependency on L to u (resp. $L^\star$ to $u^\star$) and we obtain the final equation :

$$u^\star(r,L^\star) = \frac{\rho}{V(r,L^\star)} \exp\left(-\int_{r_{min}}^{r} \frac{\sigma}{V(s,L^\star)}\mathrm{d}s\right), \tag{8}$$

yielding a coupled equation with the following equation for $L^\star$:

$$L^\star = L_0 - \int_{r_{min}}^{\infty} l(s)u^\star(s, L^\star)\mathrm{d}s. \tag{9}$$

Therefore $L^\star$ is a fixed point of the following function:

$$F(L) = L_0 - \int_{r_{min}}^{\infty} l(s)u^\star(s, L)\mathrm{d}s \tag{10}$$

with $u^\star$ as in Eq. (8). When a solution $L^\star$ is found we can insert into Eq. (8) to obtain a stationary solution.

Example 1. *When $g \equiv 1$ is constant, and l is given by (5) we obtain the explicit form for F*

$$F(L) = L_0 - \frac{4\pi\rho}{3\sigma V_l} 3\frac{f(L^\star)}{\sigma}\left(2\left(\frac{f(L^\star)}{\sigma}\right)^2 + 2r_{min}\left(\frac{f(L^\star)}{\sigma}\right) + r_{min}^2\right),$$

which is decreasing and thus admits a unique fixed point in $[0, L_0]$ whenever f is increasing with $f(0) = 0$.

Example 1 does not satisfy biological assumptions and we only include it to illustrate theoretical results. In Proposition 2, we generalize the previous example 1 for broader choices of l and g (that include biologically-sound choices) to show that indeed a unique stationary solution exists. Note that even with a simple shape for V, the solution of Eq. (9) must be found numerically.

2.3 Parameter estimation

In order to perform parameter estimation, assuming we observe adipocyte size distribution, we set the velocity according to Eqs.(6)-(7) so that

$$V(r, L) = \alpha\frac{L}{L+\kappa}\frac{r^2}{1+r^k\theta^{-k}}, \tag{11}$$

with $k \geq 2$ and from (8) the stationary solution is equal to :

$$u^\star(r, L^\star) = \rho\frac{L^\star+\kappa}{L^\star}\frac{1+r^k\theta^{-k}}{\alpha r^2}\exp\left(-\frac{\sigma}{\alpha}\frac{L^\star+\kappa}{L^\star}\left[-r^{-1} + r_{min}^{-1} + \frac{r^{k-1} - r_{min}^{k-1}}{(k-1)\theta^k}\right]\right). \tag{12}$$

We normalize Eq. (12) to 1 ($u^\star_{norm} = \frac{u^\star}{N^\star} = \frac{\sigma u^\star}{\rho}$) and we note $\sigma^\star = \frac{\sigma}{\alpha}\frac{L^\star+\kappa}{L^\star}$ (μm). The previous solution becomes

$$u^\star_{norm}(r,\sigma^\star) = \sigma^\star\left(\frac{1+r^k\theta^{-k}}{r^2}\right)\exp\left(-\sigma^\star\left[-r^{-1}+r_{min}^{-1}+\frac{r^{k-1}-r_{min}^{k-1}}{(k-1)\theta^k}\right]\right). \tag{13}$$

From Eq. (13) the solution $u^\star_{norm}$ depends on only 3 parameters, $\sigma^\star$, θ and k. Note that L^* is now considered as a parameter. Assuming L^* or L_0 as a parameter is similar, since by observing distribution of size u, and assuming l to be known (Eq.(5)), L^* only depends on parameter L_0 from Eq. (9). In addition, we notice that parameter $\sigma^\star$ is a combination of 4 parameters which cannot be estimated separately by only observing the stationary size distribution $u^\star$.

We perform an approximate Bayesian computation (ABC) [38] to estimate parameters. We use the ABC rejection sampler algorithm: first we draw a uniform distribution for the 3 parameters of interest, then we compute the L_2 error between measured and modeled cell size distributions (with the drawn parameters). We keep the vector of parameters if the L_2 error is lower than the chosen threshold and we reject it otherwise. We are considering normalized measured distributions, and for the model we use the explicit formula given by Eq. (13). This procedure is repeated 10^6 times and the threshold is set to $5\,10^{-4}$. The bounds of the uniform distributions for each parameter are the following, $k \sim \mathcal{U}(2.1, 15)$, $\sigma^\star \sim \mathcal{U}(1, 15)$ and $\theta \sim \mathcal{U}(10, 150)$. The outcome of the algorithm is a list of vector of parameters for which the L_2 error between measured and modeled cell size distributions is below the chosen threshold.

3 Results

3.1 Proof of existence, uniqueness and stability of the stationary solution

We consider here the following Partial Differential Equation (PDE) problem:

$$\begin{cases} \dfrac{\partial}{\partial t}u(t,r) + \dfrac{\partial}{\partial r}\left(V(r,L(t))u(t,r)\right) = -\sigma u(t,r), \quad r > r_{min}, \quad t > 0, \\ V(r_{min},L(t))u(t,r_{min}) = \rho, \quad t > 0, \\ L(t) = L_0 - \displaystyle\int_{r_{min}}^{\infty} l(s)u(t,s)\mathrm{d}s, \quad t > 0, \\ u(0,r) = u_0(r), \quad r > r_{min}, \end{cases} \tag{14}$$

and we take a general velocity under the form

$$V(r,L) = f(L)g(r)\,. \tag{15}$$

To begin with, we study the existence and uniqueness of the stationary solution of system (14) defined by Eq.(8)-(9).

As explained previously, we therefore look for a fixed point of function F defined at Eq. (10). In the following proposition, we prove the existence and uniqueness of the fixed point. Therefore, once L_0 is fixed, there exists a unique value for the stationary extracellular quantity of lipids $L^\star$ and a unique stationary density $u^\star$.

Proposition 2. *We assume that*

- *f is a differentiable strictly increasing function on $[0, L_0]$ with $f(0) = 0$,*
- *g is a continuous bounded positive function on $[r_{min}, +\infty)$,*
- *l is a continuously increasing function on $[r_{min}, +\infty)$ with $l(r_{min}) = 0$,*
- *for all $\lambda > 0$, $l/g \in \mathrm{L}^1\left(([r_{min}, +\infty), \exp\left(-\lambda\chi(x)\right)\mathrm{d}x\right)$, where $\chi(x) = \displaystyle\int_{r_{min}}^{x} \frac{\mathrm{d}s}{g(s)}$.*

Then, for all $L_0 > 0$, there exists a unique fixed point $L^\star \in (0, L_0)$ of function $F : [0, L_0] \to \mathbb{R}$ defined by

$$F(L) = L_0 - \int_{r_{min}}^{\infty} l(s) \frac{\rho}{g(s)f(L)} \exp\left(-\int_{r_{min}}^{s} \frac{\sigma}{g(\xi)f(L)}\mathrm{d}\xi\right)\mathrm{d}s.$$

Note that functions l, f, g given by (5)-(7)-(6) satisfy the hypotheses of Proposition 2. The proof of Proposition 2 relies on the intermediate value theorem and the fact that F is a decreasing function of L. We will make a repetitive use of the following notation

$$\chi(x) := \int_{r_{min}}^{x} \frac{1}{g(s)}\mathrm{d}s \tag{16}$$

By assumption, χ defines a diffeomorphism from $[r_{min}, \infty)$ to $[0, \infty)$, and we define

$$p(x) := l \circ \chi^{-1}(x)\,. \tag{17}$$

Proof. Thanks to notation (16), we rewrite F as:

$$F(L) = L_0 - \frac{\rho}{f(L)} \int_{r_{min}}^{\infty} \frac{l(s)}{g(s)} \exp\left(-\sigma\frac{\chi(s)}{f(L)}\right)\mathrm{d}s\,.$$

By assumption, and from Lebesgue integration theorem, F is a well defined continuous differentiable function and

- $\lim_{L\to 0} F(L) = L_0$ and
- $\lim_{L\to L_0} F(L) = L_0 - \dfrac{\rho}{f(L_0)} \displaystyle\int_{r_{min}}^{\infty} \frac{l(s)}{g(s)} \exp\left(-\sigma \frac{\chi(s)}{f(L_0)}\right) \mathrm{d}s < L_0.$

Thanks to notation (17), and using the change of variable $x = \chi(s)$, we obtain:

$$F(L) = L_0 - \frac{\rho}{f(L)} \int_0^{\infty} p(x) \exp\left(-\sigma \frac{x}{f(L)}\right) \mathrm{d}x.$$

Computing its derivative with respect to L, we have that

$$F'(L) = \rho \frac{f'(L)}{f(L)^2} \int_0^{\infty} p(x) \left(1 - \sigma \frac{x}{f(L)}\right) \exp\left(-\sigma \frac{x}{f(L)}\right) \mathrm{d}x.$$

By assumption, $f'(L) > 0$ for all $L > 0$, therefore F' has the same sign as $\displaystyle\int_0^{\infty} p(x) \left(1 - \sigma \frac{x}{f(L)}\right) \exp\left(-\sigma \frac{x}{f(L)}\right) \mathrm{d}x$. We can verify that for every L,

$$\int_0^{\infty} \left(1 - \sigma \frac{x}{f(L)}\right) \exp\left(-\sigma \frac{x}{f(L)}\right) \mathrm{d}x = 0\,.$$

As p is increasing, we can cut the integral below in two parts according to the sign of $1 - \sigma \dfrac{x}{f(L)}$:

$$\begin{aligned}
&\int_0^{\infty} p(x) \left(1 - \sigma \frac{x}{f(L)}\right) \exp\left(-\sigma \frac{x}{f(L)}\right) \mathrm{d}x \\
&= \int_0^{\frac{f(L)}{\sigma}} p(x) \left(1 - \sigma \frac{x}{f(L)}\right) \exp\left(-\sigma \frac{x}{f(L)}\right) \mathrm{d}x \\
&\qquad + \int_{\frac{f(L)}{\sigma}}^{\infty} p(x) \left(1 - \sigma \frac{x}{f(L)}\right) \exp\left(-\sigma \frac{x}{f(L)}\right) \mathrm{d}x \\
&\leq p\left(\frac{f(L)}{\sigma}\right) \int_0^{\frac{f(L)}{\sigma}} \left(1 - \sigma \frac{x}{f(L)}\right) \exp\left(-\sigma \frac{x}{f(L)}\right) \mathrm{d}x \\
&\qquad + p\left(\frac{f(L)}{\sigma}\right) \int_{\frac{f(L)}{\sigma}}^{\infty} \left(1 - \sigma \frac{x}{f(L)}\right) \exp\left(-\sigma \frac{x}{f(L)}\right) \mathrm{d}x \\
&\leq p\left(\frac{f(L)}{\sigma}\right) \int_0^{\infty} \left(1 - \sigma \frac{x}{f(L)}\right) \exp\left(-\sigma \frac{x}{f(L)}\right) \mathrm{d}x = 0.
\end{aligned}$$

We deduce that $F'(L) \leq 0$, F is continuous nonincreasing, $F(0) > 0$ and $F(L_0) < L_0$, therefore F has a unique fixed point $L^* \in (0, L_0)$. □

Now, we prove that the unique stationary solution we found is locally stable for PDE system (14), which means that the stationary solution would be the asymptotic profile of the system provided that the initial datum is taken close to the stationary solution.

Theorem 3. *We assume that :*

(H1) $f \in C^1([0, L_0])$ *is strictly increasing and* $f(0) = 0$.

(H2) $g \in C^1([r_{min}, +\infty))$, $g > 0$ *and* g *and* g' *are bounded,*

(H3) $l \in C^1([r_{min}, +\infty))$, l *is increasing with* $l(r_{min}) = 0$, *and* $\frac{l'}{1+l}$ *is bounded, Furthermore, there exist* $x_0 > 0$ *and* $K > 0$ *such that for all* $x, y \geq x_0$, $l(x + y) \leq K l(x) l(y)$,

(H4) for all $\lambda > 0$, *both* l/g *and* l' *belong to* $\mathrm{L}^1([r_{min}, +\infty), (\exp(-\lambda\chi(x))\mathrm{d}x)$.

Then the unique stationary solution of system (14) *is locally asymptotically stable in the space* $\mathrm{L}^1([r_{min}, +\infty), (1 + l(x))\mathrm{d}x)$.

Functions f, g, l given by (7)-(6)-(5) satisfy the hypotheses. We sketch here the general idea of the proof, all the details and intermediate computations are given in A.

Proof. Thanks to the separable form of the growth speed $V(r, L) = f(L)g(r)$, and using the change of variable $v(\tau, \cdot) = u(t, \cdot)$ with $\tau(t) = \int_0^t f(L(\theta))\mathrm{d}\theta$, we can show that the PDE system (14) is asymptotically equivalent to the following semilinear PDE :

$$\begin{cases} \dfrac{\partial}{\partial\tau} v(\tau, r) + \dfrac{\partial}{\partial r}\left(g(r)v(\tau, r)\right) + \dfrac{\sigma}{f(L(\tau))} v(\tau, r) = 0, \quad r > r_{min}, \tau > 0 \\ g(r_{min}) f(L(\tau)) v(\tau, r_{min}) = \rho, \quad \tau > 0, \\ L(\tau) = L_0 - \displaystyle\int_{r_{min}}^{\infty} l(r)v(\tau, r)\mathrm{d}r, \quad \tau > 0 \\ v(0, r) = u_0(r), \quad r > r_{min} \end{cases} \tag{18}$$

Eq. (18) can be written as an abstract semilinear Cauchy problem on the Banach space $X := \mathbb{R} \times \mathrm{L}^1([0, +\infty), \omega(x)\mathrm{d}x)$ for some suitable weight function ω. Then, the principle of linearized stability (Prop. 5.7.1. and 5.7.4. in [26]) allows us to reduce the stability analysis to the study of the asymptotic behaviour of the linearized problem around the stationary solution. The study of the linearized problem around $(u^\star, L^\star)$,

leads to the study of the following characteristic function Δ (see the derivation of Δ in A)

$$\Delta(\lambda) = 1 + \rho \frac{f'(L^\star)}{f^2(L^\star)} \frac{1}{\lambda} \int_0^\infty p(x) e^{-\frac{\sigma}{f(L^\star)}x} \left(\frac{\sigma}{f(L^\star)} - e^{-\lambda x} \left(\lambda + \frac{\sigma}{f(L^\star)} \right) \right) \mathrm{d}x \,,$$

where we recall that p is defined in notation (17). Finally, we show that if the characteristic function Δ has no root with non-negativereal part, then the unique stationary solution of (14) is locally asymptotically stable. Now, let us remark that $\lambda \neq 0$ and $\Delta(\lambda) = 0$ is equivalent to:

$$\lambda = \rho \frac{f'(L^\star)}{f^2(L^\star)} \int_0^\infty p(x) e^{-\frac{\sigma}{f(L^\star)}x} \left(e^{-\lambda x} \left(\lambda + \frac{\sigma}{f(L^\star)} \right) - \frac{\sigma}{f(L^\star)} \right) \mathrm{d}x \,. \tag{19}$$

For the sake of brevity, we set $\lambda_0 := \frac{\sigma}{f(L^\star)}$. Then Eq. (19) can be rewritten as:

$$\begin{aligned} \frac{f^2(L^\star)}{\rho f'(L^\star)} \lambda &= \int_0^\infty p(x) e^{-\lambda_0 x} \left(e^{-\lambda x} \left(\lambda + \lambda_0 \right) - \lambda_0 \right) \mathrm{d}x \\ &= \int_0^\infty p(x) e^{-(\lambda_0 + \lambda)x} \left(\lambda + \lambda_0 \right) \mathrm{d}x - \lambda_0 \int_0^\infty p(x) e^{-\lambda_0 x} \mathrm{d}x \,. \end{aligned}$$

By integration by parts (and using $p(0) = 0$ by (H3)), we get:

$$\begin{aligned} \frac{f^2(L^\star)}{\rho f'(L^\star)} \lambda &= \int_0^\infty p'(x) e^{-(\lambda_0 + \lambda)x} \mathrm{d}x - \int_0^\infty p'(x) e^{-\lambda_0 x} \mathrm{d}x \\ &= \int_0^\infty p'(x) e^{-\lambda_0 x} \left(e^{-\lambda x} - 1 \right) \mathrm{d}x \,. \end{aligned}$$

Using the complex decomposition of $\lambda = \Re(\lambda) + i\Im(\lambda)$, and taking the real part of the later equation, we obtain:

$$\frac{f^2(L^\star)}{\rho f'(L^\star)} \Re(\lambda) = \int_0^\infty p'(x) e^{-\lambda_0 x} \left(\cos(\Im(\lambda)x) e^{-\Re(\lambda)x} - 1 \right) \mathrm{d}x \,.$$

From (H1), since $L^\star \neq 0$, $\dfrac{f^2(L^\star)}{\rho f'(L^\star)} > 0$.

If $\Re(\lambda) > 0$, by $(H2)$ and $(H3)$, p is increasing, thus:

$$\int_0^\infty p'(x) e^{-\lambda_0 x} \left(\cos(\Im(\lambda)x) e^{-\Re(\lambda)x} - 1 \right) \mathrm{d}x \leq 0 \,,$$

leading to a contradiction.

If $\Re(\lambda) = 0$, the equation above leads to $\Im(\lambda) = 0$ which is impossible since $\lambda \neq 0$.

Therefore, there is no root with non-negative real part.

□

3.2 Numerical simulations

We perform now several numerical experiments, using the presented model with functions l, f, g given by (5)-(7)-(6). First, we explore the effect of the total lipid quantity L_0 by computing the stationary solution defined by the coupling (9)-(12). In the left panel of Fig. 1, we represent distributions for three values of L_0. To be able to compare the different graphs, we start the radius value at 25 μm in the plots. An increase in total lipids L_0 increases the lipid volume inside cells whereas the distribution of size remains bimodal.

Fig. 1 right panel displays a log-log plot of the extracellular lipids $L^\star$ and of the stationary amount of intracellular lipids $L^\star_{\text{int}} := \int_{r_{min}}^{\infty} \frac{4\pi}{3V_l}(s^3 - r_{min}^3)u^\star(s)\mathrm{d}s$ (see Eq. (3)), as a function of L_0. For low values of L_0, the resulting extracellular lipid quantity $L^\star$ is small and almost constant. Moreover, the amount of lipids inside the cells $L^\star_{\text{int}}$ increases linearly with respect to L_0 and also $L^\star$, since $L_0 = L^\star + L^\star_{\text{int}}$. Thanks to a linear regression we compute the coefficient of this linear increase and we find it equal to 1. Thus, the uptake of lipids by the cells occurs proportionally to the amount of available lipid L_0. We notice that above a certain value of L_0, a plateau is reached for the intracellular lipids amount, corresponding to the maximal lipid amount the tissue can store. For values above this threshold value of L_0, the intracellular lipid amount does not increase any more and therefore the extracellular lipids start to accumulate (increase of $L^\star$).

Now, we will perform in Section 3.3 a data fitting procedure using the normalized stationary solution (13) and we will estimate the 3 parameters: k, θ and $\sigma^\star$. Therefore, in Fig. 2, we show the effect of varying these 3 parameters on the shape of the normalized stationary solution (13). The top left panel of Fig. 2 shows the dependency on k coefficient which impacts mostly the right hand mode. It plays a role on the position and the height of the right hand mode. For the chosen parameters, we can see that $k = 3$ is not sufficient to obtain bimodality and this is a notable difference with the previous model proposed in [36]. Fig. 2 top right panel shows the influence of parameter θ on the size distribution. Similarly to k it impacts the position and height of the right mode. We can say that parameter θ mostly represents the nadir (lowest point between the two modes) of the size distribution. Finally, Fig. 2 bottom left panel shows the dependency with respect to $\sigma^\star$. It has a huge overall impact on the distribution since $\sigma^\star$ corresponds to the ratio between the cell death rate σ and the growth rate coefficient $\alpha\frac{L^\star}{L^\star+\kappa}$. Parameter $\sigma^\star$ impacts both small and large size frequency.

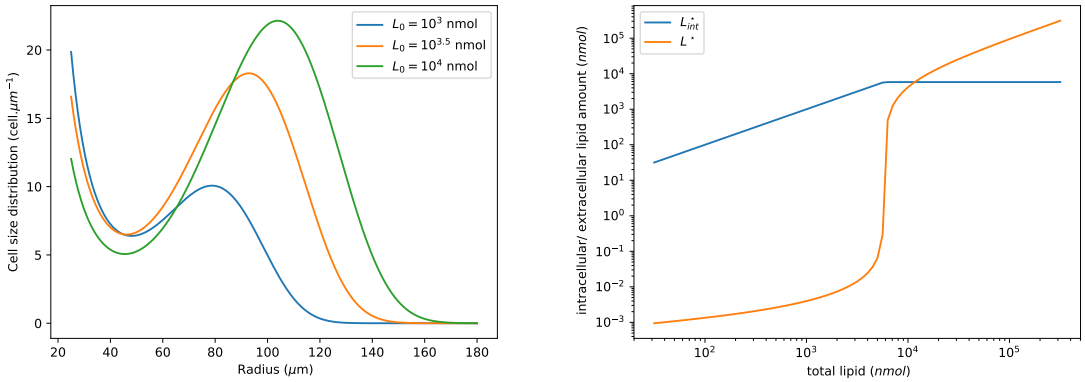

Figure 1: Effect of total lipid quantity on stationary solution. Left panel: plot of stationary solution (9)-(12) for three values of L_0 (to obtain visually comparable graphs the radii r start at $25\mu m$). Right panel: log-log plot of the extracellular lipid $L^\star$ (orange) and intracellular lipid amount $L^\star_{\text{int}}$ (blue) with respect to L_0. Parameters are: $V_l = 1.091.10^6 \mu\text{m}^3.\text{nmol}^{-1}$, $\alpha = 10^{-4}\mu\text{m}^{-1}.\text{time}^{-1}$, $\theta = 50\mu\text{m}$, $\sigma = 5.10^{-4}$ time^{-1}, $\rho = 1\text{cell.time}^{-1}$, $k = 6$, $\kappa = 10^{-2}$ nmol, $r_{min} = 10\mu\text{m}$.

3.3 Comparison between modeled and measured cell size distributions

A general fitting approach is not the goal of this article. Instead, we want to assess if this new model produces accurate distributions. We randomly select four adipose size distributions from our database: retro-peritoneal adipose tissue of male Wistar rats from different experiments [15, 35]. The code and the data files to perform the estimations are available here: https://plmlab.math.cnrs.fr/audebert/adipocyte_rapid_turnover_modeling.

The ABC rejection sampler algorithm is applied to each selected data set. The selection rates are low, as expected with this method [38], and the number of selected parameter vectors varies from 52 to 1524. The posterior distributions have a Gaussian shape and are far from the bounds of the prior uniform distributions (Fig. 5). The estimated parameters are chosen as the mean of the selected list of parameters, we also computed the standard deviation. Table 1 sums up the estimated values for the four animals. The small standard deviations show the robustness of the parameter estimation. In addition, the estimated parameters do not vary wildly between data sets. Fig. 3 shows that the model can well approximate measured distributions.

Considering that adipocyte death follows a linear decay with parameter σ in Eq. (1), individual adipocyte turnover time is therefore on average equal to $1/\sigma$.

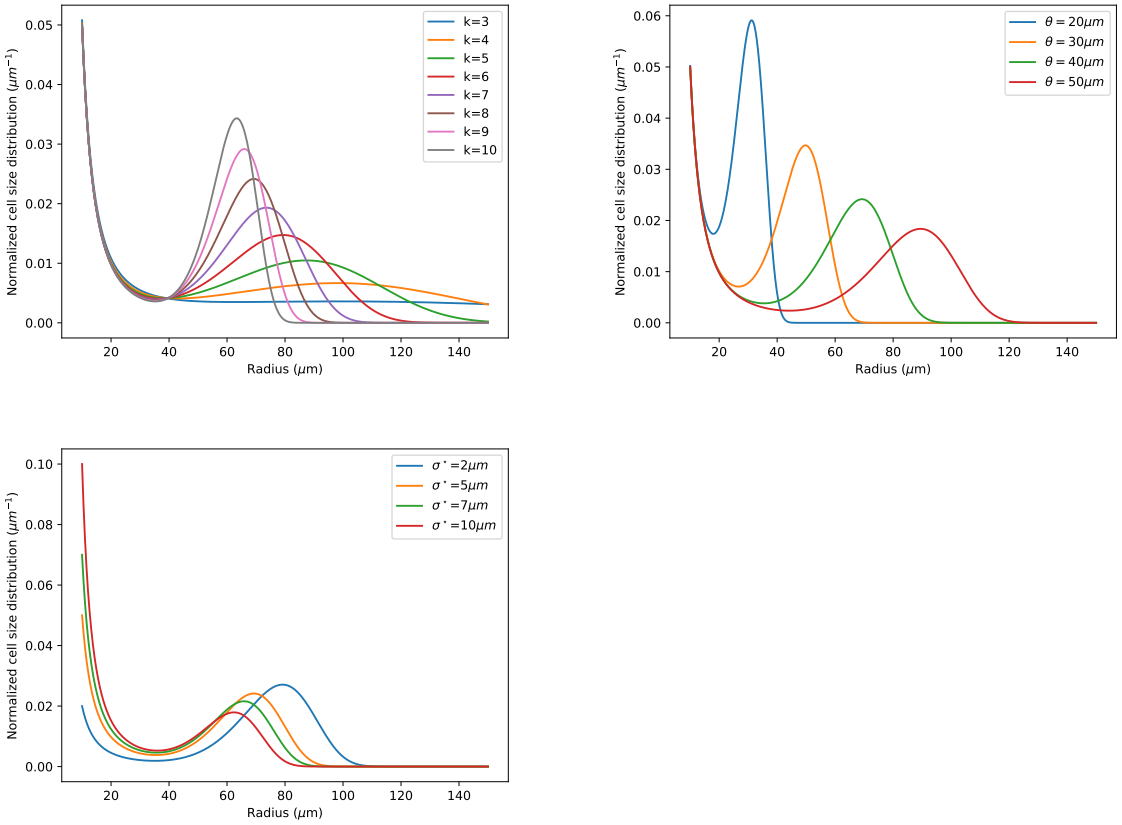

Figure 2: Sensitivity to parameters of stationary solution defined in equation (13). Top left : dependency of the stationary solution with respect to parameter k. Top right: impact of θ parameter on the stationary solution. Bottom left: impact of $\sigma^\star$ parameter on the stationary solution. Default parameters are: $k = 8$, $\theta = 40\mu$m, $\sigma^\star = 5\mu$m, $r_{min} = 10\mu$m.

animal	$\sigma^\star$ (μm)	θ (μm)	k
rat 1	6.24 ± 0.6	33.7 ± 2.15	6.08 ± 0.7
rat 2	7.58 ± 0.81	30.33 ± 4.37	3.82 ± 0.72
rat 3	5.28 ± 0.24	43.07 ± 0.78	9.26 ± 0.38
rat 4	6.03 ± 0.73	42.87 ± 3.09	7.55 ± 1.06

Table 1: Estimations obtained with ABC rejection sampler. The mean and standard deviation of the selected list of parameters are presented for each animal. The procedure is repeated 10^6 times and the threshold is set to $5\,10^{-4}$.

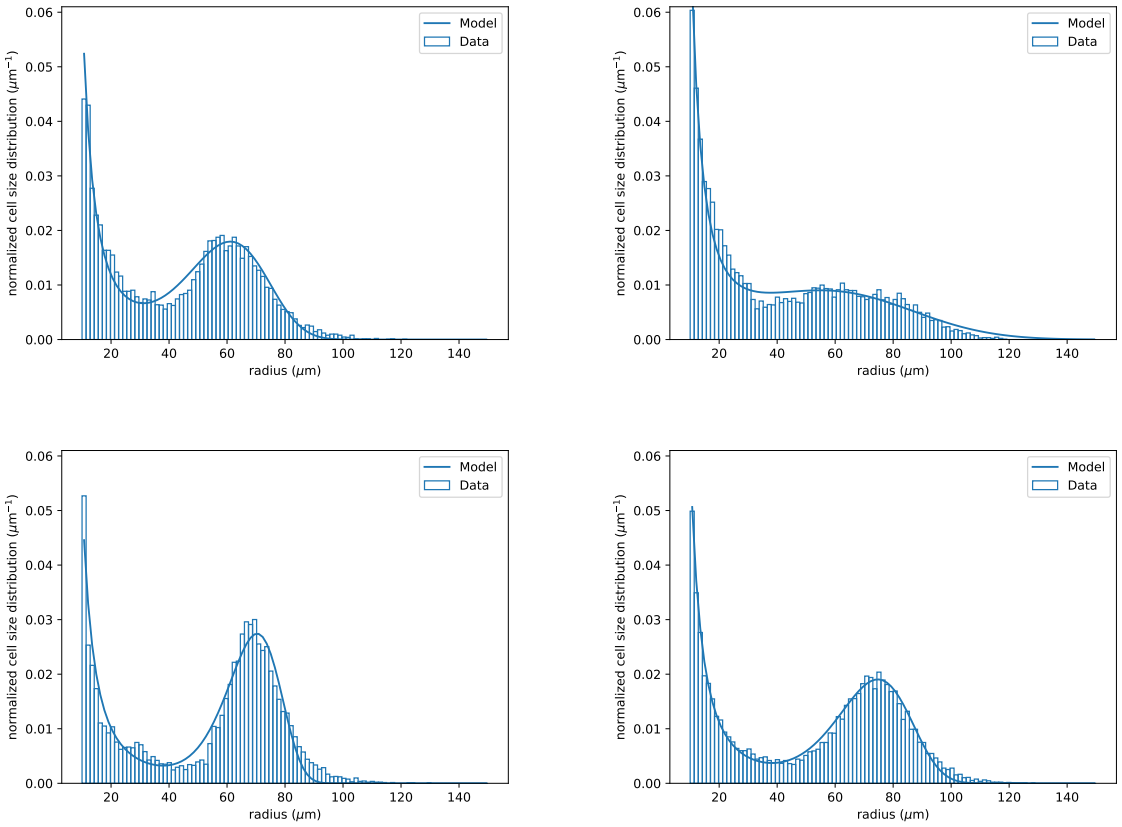

Figure 3: Model compared to measurements for four different male Wistar rats cell size distributions [15, 35]. Table 1 sums up the parameters, and the model is described by Eq. (13). Data are represented with histograms and the model output with solid lines.

animal	$\alpha^\star_{115}$ (μm^{-1}.day^{-1})	$\bar{V}_{115}$ (μm.day^{-1})	$\alpha^\star_{45}$ (μm^{-1}.day^{-1})	$\bar{V}_{45}$ (μm.day^{-1})
rat 1	0.0014	0.2897	0.0036	0.7403
rat 2	0.0011	0.2859	0.0029	0.7308
rat 3	0.0016	0.3537	0.0042	0.9039
rat 4	0.0014	0.3585	0.0037	0.9162

Table 2: Lipid uptake rate and average velocity. Parameter $\alpha^\star$ and average velocity ($\int_{r_{min}}^{r_{max}} V(x)u^\star_{norm}(x)dx$) are computed with estimations from literature for $1/\sigma$ and ABC rejection algorithm for the other parameters (Table 1). The subscript $._{115}$ corresponds to the computation for a turnover of 115 days and $._{45}$ for a turnover of 45 days.

We know from literature that 0.6% to 1.5% adipocytes are replaced each day for lean mice ad libitum [30, 29, 19]. This corresponds to a turnover ranging from 45 days to 115 days. Those estimations enable also to fix the time unit to day (before it was an arbitrary time unit). From the estimated values for $\sigma^\star$ we can compute an estimate of the velocity rate $\alpha^\star$, defined by

$$\alpha^\star = \alpha \frac{L^\star}{L^\star + \kappa} = \frac{\sigma}{\sigma^\star}\, \mu\text{m}^{-1}.\text{day}^{-1}.$$

Under these assumptions, lower ($\alpha^\star_{115}$) and upper ($\alpha^\star_{45}$) bounds for the rate $\alpha^\star$ can be estimated for each rat. These estimations are summed up in Table 2. From the estimation of $\alpha^\star$ we can also compute lower and upper bounds of velocities with respect to radius (Eq. (11)). Left panel of Fig. 4 shows the velocity for rat 4 assuming 45 or 115 days for adipocyte turnover. For 45 day turnover the velocity increases faster and higher with respect to radius. In addition we compute the averaged velocity ($\bar{V} = \int_{r_{min}}^{r_{max}} V(x)u^\star_{norm}(x)dx$) with lower and upper bound of $\alpha^\star$ and the estimated parameters for each animal (Table 2). Under our assumptions, the velocity ranges from 0.28 to 0.9 μm.day^{-1}. Right panel of Fig. 4 shows for rat 4 the trajectory of two cells with initial radius of 10μm and highest and lowest estimated velocities. It shows a rapid increase in size for the upper bound of the velocity that then slows down. Whereas the cell with the lower bound velocity shows a similar dynamics with a smaller velocity, and it ends with a lower cell size.

4 Discussion

We provided a new dynamical model of adipocyte size distributions. The model assumptions are different from the models we previously proposed [36, 35, 28, 9, 6].

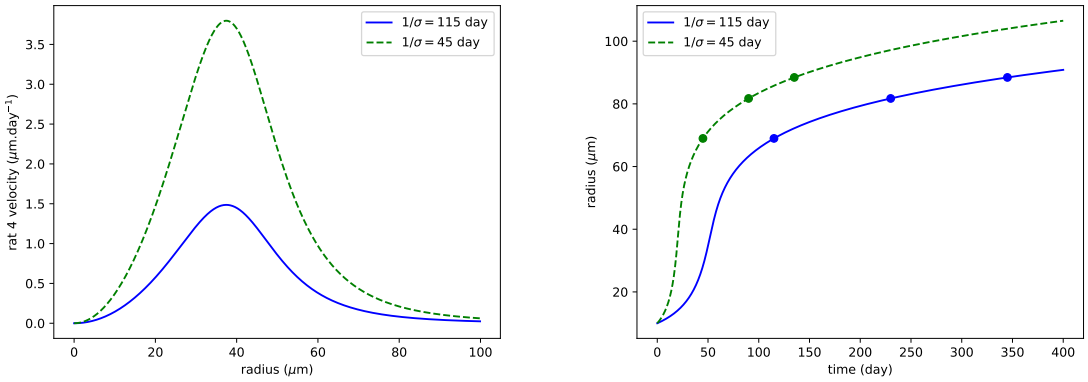

Figure 4: Example of velocity function V and cell radius trajectories. Left panel shows velocity functions (Eq. (11)) with respect to radius computed for both turnover times and with the estimated parameter values of rat 4 (Tables 1 and 2). Right panel shows cell trajectory with velocity estimated for rat 4 with 45 and 115 days for adipocyte turnover. Initially $r(0) = 10\mu$m and the curve is computed with explicit Euler scheme $r_{k+1} = r_k + dtV(r_k)$ and $dt = 0.01$ day. Dots point out the cell radius after $1/\sigma$, $2/\sigma$ and $3/\sigma$ days in each case.

Previously the transport term in the equation described lipid exchanges and the two modes of the stationary solution were corresponding to the equilibrium between lipogenesis and lipolysis (the zeros of the transport term). Here, cells are constantly growing in size, and when growth is slowed for a certain size, cells tend to accumulate at this size. This is called a "toll effect", when toll gate slows down cars, leading to an increase of local density. The growth velocity is tailored to obtain the desired shape of the cell size distribution. However, we stress that this velocity remains a realistic description of the fluxes for adipocyte size growth. Indeed, the size velocity is proportional to the cell surface and starts slowly at r^2 rate [35, 14, 34]. The rate will increase until the tissue prevents the cell growth and then velocity for large size drops close to zero. The resulting cell size distribution yields in bimodal distribution i.e accumulation around the size of low growth speed for small and large enough radius. The accumulation at right tail (low growth speed) is prevented by cell death. To conclude, with a constant inflow of cells, cell death, and cells that continually increase in size we can obtain extremely realistic cell size distributions.

We have also proved that the proposed model admits a unique stationary solution, locally asymptotically stable, for a wide choice of problem functions. This justifies the data fitting procedure with the stationary solution. The key assumption that enables the study of the long-time behavior of the model is the separability of the adipocyte

growth speed into two distinct functions: one depending only on the extracellular lipid amount, and the other only on the cell radius. The mathematical analysis of the long-term behavior of general size-structured population models is known to be particularly challenging. However, when the growth rate has a separable form, an implicit time-rescaling transformation can be employed to eliminate the nonlinearity in the growth velocity. This transformation allows the model to be rewritten as a semilinear abstract Cauchy problem, to which well-established stability results can be applied [26]. To our knowledge, this strategy has been successfully applied in the context of erythropoiesis modeling [10, 11] and oogenesis modeling [4]. In our context, in addition to the separability assumption, the existence of a unique locally stable steady state mainly relies on two biologically natural assumptions: (i) adipocytes grow faster when more extracellular lipid is available, and (ii) the amount of lipids stored in an adipocyte increases with its size.

The measured and simulated cell size distributions are in good agreement. The proposed model reproduces most of the features we expect to obtain: bimodal distribution, cell size spanning, large cell modes increasing with increased lipid input. We obtain the same properties as the previous model [36, 6], a maximum storage volume for the tissue. When this maximum volume is reached extracellular lipids accumulate as it did in the previous model. Our modeling assumption presents some limitations. The death rate is constant and does not depend on cell size, which might be unrealistic. Indeed, increased death rate has been associated with increased adipocyte size and in obesity an increased turnover has been reported [3, 12]. The proposed model only considers a constant recruitment of new adipocytes. Assuming the recruitment of adipocytes is varying with for example time, extracellular lipids or intracellular lipids may enable to explore the trade-off between hyperplasia (increase cell number) and hypertrophy (increase cell size) to manage lipid storage [31].

Other authors have proposed models with adipocytes continually increasing in size [17, 16]. However, the growth velocity and the death terms are more complex, not mechanically related and described by several parameters. One of the true advantages of the model proposed here is the explicit form for a normalized stationary solution that is parameterized by three parameters. The fit with the three parameters function that we proposed is robust, and well-posed in the sense that a fit will lead to a unique set of parameters. In addition, one of the parameters (θ) automatically gives an estimate of the nadir. We have performed an ABC rejection algorithm that can be computationally costly if the cost function is slow to compute. Here, with the explicit form of $u^\star_{norm}$ (Eq. (13)) the estimations were very fast. This explicit function gives a new way to fit adipocyte size distributions with only three parameters, whereas, in past works, distributions of adipocyte sizes have been fitted with two exponential functions and a Gaussian, yielding in at least 6 parameters [27, 17, 35].

This model presents a novel and simple view of the adipocyte size distribution as

a stationary distribution of ever growing (albeit dying) cells. In accordance with our previous models, it does not suppose any cell subpopulations, but does not need any individual cell variation [36, 6] or diffusion term [9, 28]. Compared to the previous models where age structure was not related to size, this model links the age of the cells and their size. This hypothesis could certainly be tested with real experiments to distinguish between the two models.

5 Acknowledgments

The authors acknowledge the support of the French Agence Nationale de la Recherche (ANR), under MATIDY grant ANR-20-CE45-0003-01.

A Proof of theorem 3

We will first show that Eq. (18) can be written as an abstract non-densely defined semilinear Cauchy problem on the Banach space $X := \mathbb{R} \times \mathrm{L}^1([0, +\infty), \omega(x)\mathrm{d}x)$ for some suitable weight function ω. Then, the principle of linearized stability, stated in [26] (see Prop. 5.7.1. and Prop. 5.7.4.) for these problems, allows us to reduce the stability analysis to the study of the asymptotic behavior of the linearized problem around the stationary solution, under some regularity hypothesis on the model parameters. We then study the asymptotic behavior of the linearized problem thanks to arguments from linear semigroup theory.

For the reader's convenience, we recall here the assumptions (H1)-(H4) of Theorem 3 :

(H1) $f \in C^1([0, L_0])$ is strictly increasing and $f(0) = 0$.

(H2) $g \in C^1([r_{min}, +\infty))$, $g > 0$ and g and g' are bounded,

(H3) $l \in C^1([r_{min}, +\infty))$, l is increasing with $l(r_{min}) = 0$, and $\frac{l'}{1+l}$ is bounded, Furthermore, there exist $x_0 > 0$ and $K > 0$ such that for all $x, y \geq x_0$, $l(x + y) \leq K l(x) l(y)$,

(H4) for all $\lambda > 0$, both l/g and l' belong to $\mathrm{L}^1([r_{min}, +\infty), (\exp(-\lambda\chi(x))\mathrm{d}x)$.

From proposition 2, we know that $L^\star \neq 0$. Let $\varepsilon > 0$ such that $L^\star > \varepsilon$. As we consider the local stability of the stationary solution, we can replace f by a function $\tilde{f}$ defined on $\mathbb{R}$ such that $\tilde{f} \geq f(\varepsilon/2) > 0$, $\tilde{f} \in C^1(\mathbb{R})$ and $f \equiv \tilde{f}$ on $[\varepsilon, +\infty)$. This trick does not change the stationary solution and its local stability, and this simplifies the formalization of the abstract Cauchy problem. In what follows, $\tilde{f}$ is denoted by f to ease the notation.

With arguments similar to those in section 3 of [4], we can check that the stationary solution $v^\star$ of (18) is equal to the stationary solution $u^\star$ of (14), and, as f is a differentiable strictly increasing function on $[0, L_0]$ that the local $\mathrm{L}^1([r_{min}, +\infty), (1 + l(x))\mathrm{d}x)$-stability (resp. local asymptotic stability) of $u^\star$ is equivalent to the local $\mathrm{L}^1([r_{min}, +\infty), (1 + l(x))\mathrm{d}x)$-stability (resp.local asymptotic stability) of $v^\star$. This time-scaling transformation removes the nonlinear part of the growth rate, so that the long-time behavior of (14) can be studied using results from semilinear equation theory.

As g is positive, we can also do the change of space variable

$$x = \chi(r) := \int_{r_{min}}^{r} \frac{1}{g(s)} \mathrm{d}s \tag{20}$$

and $w(\tau, x) = v(\tau, r)$ to obtain the following problem on w:

$$\begin{cases} L(\tau) = L_0 - \int_0^\infty k(x) w(\tau, x) \mathrm{d}x, \quad \tau > 0 \\ \partial_\tau w(\tau, x) + \partial_x w(\tau, x) + \left(m(x) + \frac{\sigma}{f(L(\tau))} \right) w(\tau, x) = 0, \quad x > 0, \tau > 0 \\ g(r_{min}) f(L(\tau)) w(\tau, 0) = \rho, \quad \tau > 0 \\ w(0, x) = w_0(x), \quad x > 0 \end{cases} \tag{21}$$

where $m = g' \circ \chi^{-1}$, $w_0 = u_0(\chi^{-1}(x))$ and $k = (l \circ \chi^{-1}) \times (g \circ \chi^{-1})$. Then the local $\mathrm{L}^1([r_{min}, +\infty), (1 + l(x))\mathrm{d}x)$-stability (resp. local asymptotic stability) of $u^\star$ is equivalent to the local $\mathrm{L}^1([0, +\infty), \omega(x)\mathrm{d}x)$-stability (resp. local asymptotic stability) of $w^\star$, the stationary solution of (21), given by $w^\star = u^\star \circ \chi^{-1}$, where the weight ω is defined by :

$$\omega(x) := g(1 + l) \circ \chi^{-1}. \tag{22}$$

We consider the Banach space $X := \mathbb{R} \times \mathrm{L}^1([0, +\infty), \omega(x)\mathrm{d}x)$ endowed with the norm

$$\|(a, \phi)\|_X := |a| + \frac{1}{\omega(0)} \|\phi\|_{\mathrm{L}^1((0,+\infty), \omega(x)\mathrm{d}x)} = |a| + \frac{1}{\omega(0)} \int_0^\infty \omega(x) \, |\phi(x)| \, \mathrm{d}x \, .$$

Let us remark that by (H4) and Eq. (8) we can see that $u^\star \in \mathrm{L}^1([r_{min}, +\infty), (1 + l(x))\mathrm{d}x)$, so that $w^\star \in L^1([0, +\infty), \omega(x)dx)$ and $(0, w^\star) \in X$.

Let us define the following linear operator $A : D(A) \subset X \to X$ by

$$A \begin{pmatrix} 0 \\ \phi \end{pmatrix} = \begin{pmatrix} -\phi(0) \\ -\partial_x \phi \end{pmatrix}, \quad D(A) = \{0\} \times \left(\mathrm{L}^1([0, +\infty), \omega(x)\mathrm{d}x) \cap W^{1,1}([0, +\infty), \mathrm{d}x) \right) \tag{23}$$

and the map $G : \overline{D(A)} = \{0\} \times \mathrm{L}^1([0,+\infty), \omega(x)\mathrm{d}x) \to X$ by

$$G\begin{pmatrix} 0 \\ \phi \end{pmatrix} = \begin{pmatrix} R(\phi) \\ M(\phi) \end{pmatrix}.$$

with

$$R(\phi) := \frac{\rho}{g(r_{min}) f(L_0 - \int_0^\infty k(x)\phi(x)\mathrm{d}x)},$$

and

$$M(\phi) = -m\phi - \frac{\sigma}{f(L_0 - \int_0^\infty k(x)\phi(x)\mathrm{d}x)}\phi.$$

Then (21) can be written as the following semilinear abstract Cauchy problem :

$$\begin{cases} \frac{d\mathbf{w}(\tau)}{d\tau} = A\mathbf{w}(\tau) + G(\mathbf{w}(\tau)), \quad \tau > 0 \\ \mathbf{w}(0) = \begin{pmatrix} 0 \\ w_0 \end{pmatrix} \in \overline{D(A)}, \end{cases} \tag{24}$$

with $\mathbf{w} = \begin{pmatrix} 0 \\ w \end{pmatrix}$. Moreover, the map G is continuously differentiable around $\mathbf{w}^\star$ and the linearized problem around stationary solution $\mathbf{w}^\star = \begin{pmatrix} 0 \\ w^\star \end{pmatrix}$ is given by :

$$\frac{d\mathbf{w}(\tau)}{d\tau} = A\mathbf{w}(\tau) + DG(\mathbf{w}^\star)\mathbf{w}(\tau),\ \tau \geq 0,\ \mathbf{w}(0) = \mathbf{w_0} \in \overline{D(A)},$$

where $DG(\mathbf{w}^\star) \in \mathcal{L}(\overline{D(A)}, X)$ is the Fréchet derivative of G at $\mathbf{w}^\star$, and is given explicitly as:

$$DG(\mathbf{w}^\star)\begin{pmatrix} 0 \\ \phi \end{pmatrix} = \begin{pmatrix} \frac{\rho}{g(r_{min})} \frac{f'(L^\star)}{f(L^\star)^2} \int_0^\infty k(x)\phi(x)\mathrm{d}x \\ \left(-\sigma \frac{f'(L^\star)}{f(L^\star)^2} \int_0^\infty k(x)\phi(x)\mathrm{d}x\right) w^\star - \left(\frac{\sigma}{f(L^\star)} + m\right)\phi \end{pmatrix}, \tag{25}$$

with $L^* = L_0 - \int_0^\infty k(x)w^*(x)dx$.

Proposition 4. *Let assumptions (H1)-(H4) hold. Then A defined by (23) is a closed Hille-Yosida operator. Furthermore, let $\mathbf{w}^\star$ a stationary solution of (24), then the essential growth bound of $(A + DG(\mathbf{w}^\star))_{\overline{D(A)}}$ is strictly negative.*

Proof. First of all, let us show that A is a Hille-Yosida operator. Consider $\Re\lambda > 0$, and $(a, \psi) \in X$:

$$(\lambda\mathbb{I} - A)^{-1}\begin{pmatrix} a \\ \psi \end{pmatrix} = \begin{pmatrix} 0 \\ \phi \end{pmatrix} \Leftrightarrow \begin{cases} \phi(0) = a \\ \phi' + \lambda\phi = \psi \end{cases}$$
$$\Leftrightarrow \phi(y) = ae^{-\lambda y} + \int_0^y \psi(s)e^{-\lambda(y-s)}\mathrm{d}s,\ y \in [0,+\infty).$$

We can compute

$$\left\|(\lambda\mathbb{I}-A)^{-1}\begin{pmatrix}a\\ \psi\end{pmatrix}\right\|_X = \left\|\begin{pmatrix}0\\ \phi\end{pmatrix}\right\|_X = |0| + \frac{1}{\omega(0)}\int_0^\infty \|\phi\|_{L^1([0,+\infty),\omega(x)\mathrm{d}x)}$$
$$\leq \frac{1}{\omega(0)}\int_0^\infty |a|\, e^{-\lambda y}\omega(y)\mathrm{d}y + \frac{1}{\omega(0)}\int_0^\infty \omega(y)\int_0^y |\psi(s)|e^{-\lambda(y-s)}\mathrm{d}s\mathrm{d}y\,,$$
$$\leq \frac{|a|}{F(\lambda,0)}\int_0^\infty F(\lambda,y)\mathrm{d}y + \frac{1}{\omega(0)}\int_0^\infty |\psi(s)|\omega(s)\frac{1}{F(\lambda,s)}\int_s^\infty F(\lambda,y)\mathrm{d}y\mathrm{d}s\,,$$

with $F(\lambda,x) := \omega(x)e^{-\lambda x}$. We need the following lemma

Lemma 5. *If for some $\lambda_1 > 0$, $x \mapsto F(\lambda_1,x) = \omega(x)e^{-\lambda_1 x}$ is decreasing on $[0,+\infty)$, then for all $\lambda > \lambda_1$ and all $s \geq 0$, $\dfrac{1}{F(\lambda,s)}\displaystyle\int_s^\infty F(\lambda,y)\mathrm{d}y \leq \frac{1}{\lambda-\lambda_1}$.*

Proof of lemma 5. We notice that $\dfrac{F(\lambda,y)}{F(\lambda_1,y)} = e^{-(\lambda-\lambda_1)y}$ and by assumption, for all $y \geq s \geq 0$, $\dfrac{F(\lambda_1,y)}{F(\lambda_1,s)} \leq 1$, therefore for $\lambda > \lambda_1$ and $s \geq 0$,

$$\frac{1}{F(\lambda,s)}\int_s^\infty F(\lambda,y)\mathrm{d}y \leq e^{(\lambda-\lambda_1)s}\int_s^\infty e^{-(\lambda-\lambda_1)y}\mathrm{d}y = \frac{1}{\lambda-\lambda_1}.$$

□

Now, let us verify that $x \to F(\lambda_1,x)$ is decreasing for some λ_1. We have $\partial_x F_1(\lambda_1,x) = \omega'(x)e^{-\lambda_1 x} - \lambda_1\omega(x)e^{-\lambda_1 x}$, so $\partial_x F_1(\lambda_1,x) \leq 0$ if and only if $\lambda_1 \geq \frac{\omega'(x)}{\omega(x)}$. With the definition (22) of ω and (20) of χ, we have :

$$\frac{\omega'}{\omega} = \left(g' + g\frac{l'}{1+l}\right)\circ\chi^{-1}$$

and by assumptions (H2) and (H3), g' and $g\frac{l'}{1+l}$ are bounded, so we can choose λ_1 such that for all $x \geq 0$, $\lambda_1 \geq \frac{\omega'(x)}{\omega(x)}$. Finally, using lemma 5,

$$\left\|(\lambda\mathbb{I}-A)^{-1}\begin{pmatrix}a\\ \psi\end{pmatrix}\right\|_X \leq \frac{1}{\lambda-\lambda_1}\left(|a| + \frac{1}{\omega(0)}\int_0^\infty |\psi(s)|\omega(s)ds\right) \leq \frac{\left\|\begin{pmatrix}a\\ \psi\end{pmatrix}\right\|_X}{\lambda-\lambda_1}\,.$$

So for all $\lambda > \lambda_1$,

$$\left\|(\lambda\mathbb{I}-A)^{-1}\right\|_{\mathcal{L}(X)} \leq \frac{1}{\lambda-\lambda_1},$$

hence, for all $n \geq 1$,

$$\left\|(\lambda \mathbb{I} - A)^{-n}\right\|_{\mathcal{L}(X)} \leq \left\|(\lambda \mathbb{I} - A)^{-1}\right\|^n_{\mathcal{L}(X)} \leq \frac{1}{(\lambda - \lambda_1)^n}\,,$$

and $\lambda \in \rho(A)$, the resolvent set of A, so A is a Hille-Yosida operator.

From Eq. (25), we can write $DG(\mathbf{w}^\star)$ as the sum of two linear operators :

$$DG(\mathbf{w}^\star)\begin{pmatrix}0\\ \phi\end{pmatrix} = B\begin{pmatrix}0\\ \phi\end{pmatrix} + C\begin{pmatrix}0\\ \phi\end{pmatrix}$$

where $B : \overline{D(A)} \to X$ is the bounded linear operator defined by

$$B\begin{pmatrix}0\\ \phi\end{pmatrix} = \begin{pmatrix}0\\ -(\frac{\sigma}{f(L^\star)} + m)\phi\end{pmatrix}$$

and $C : \overline{D(A)} \to X$ is defined by

$$C\begin{pmatrix}0\\ \phi\end{pmatrix} = P(\phi)\begin{pmatrix}\frac{\rho}{g(r_{min})}\frac{f'(L^\star)}{f(L^\star)^2}\\ -\sigma\frac{f'(L^\star)}{f(L^\star)^2}w^\star\end{pmatrix}\,, \tag{26}$$

where we define the linear map $P : \mathrm{L}^1([0,+\infty), \omega(x)\mathrm{d}x) \to \mathbb{R}$ by

$$P(\psi) = \int_0^\infty k(x)\psi(x)\mathrm{d}x, \quad \forall \psi \in \mathrm{L}^1([0,+\infty), \omega(x)\mathrm{d}x)\,. \tag{27}$$

By the Riesz-Fréchet-Kolmogorov theorem, P defined by Eq. (27) is a compact bounded linear operator. As A is a Hille-Yosida operator, B is bounded linear and C is compact bounded linear, we can apply Th. 1.2. in [7] to state that the essential growth bound of $(A + DG(\mathbf{w}^\star))_{\overline{D(A)}} = (A + B + C)_{\overline{D(A)}}$ is less than or equal to the essential growth bound of $(A + B)_{\overline{D(A)}}$. Furthermore, the essential growth bound (corollary IV.2.10 in [8]) of $(A + B)_{\overline{D(A)}}$ is less than or equal to the growth bound of $(A + B)_{\overline{D(A)}}$. Let us show that the growth bound of $(A + B)_{\overline{D(A)}}$ is negative. Using the characteristic method, we show that $(A+B)_{\overline{D(A)}}$ generates a C^0-semigroup $\{T_{(A+B)_{\overline{D(A)}}}(t)\}_{t\geq 0}$ on $\overline{D(A)}$ defined by

$$T_{(A+B)_{\overline{D(A)}}}(t)\begin{pmatrix}0\\ \phi\end{pmatrix} = \begin{pmatrix}0\\ \hat{T}_{(A+B)_{\overline{D(A)}}}(t)(\phi)\end{pmatrix}$$

where :

$$\hat{T}_{(A+B)_{\overline{D(A)}}}(t)(\phi)(x) = \begin{cases}\phi(x-t)e^{-\int_{x-t}^x m(y)+\frac{\sigma}{f(L^\star)}\mathrm{d}y} & \text{if } x \geq t,\\ 0 & \text{otherwise.}\end{cases}$$

In order to compute the norm of $T_{(A+B)_{\overline{D(A)}}}(t)$ thereafter, we need the following expression :

$$\exp\left(-\int_\xi^x m(y)dy\right) = \exp\left(-\int_\xi^x g'\circ\chi^{-1}(y)dy\right) = \frac{g\circ\chi^{-1}(\xi)}{g\circ\chi^{-1}(x)}, \tag{28}$$

coming from the change of variable $z=\chi^{-1}(y)$ in the integral and the expression (20) of χ.

Then,

$$\left\|T_{(A+B)_{\overline{D(A)}}}(t)\begin{pmatrix}0\\ \phi\end{pmatrix}\right\|_X = \frac{1}{\omega(0)}e^{-t\frac{\sigma}{f(L^\star)}}\int_t^\infty \omega(x)\,|\phi(x-t)|\,e^{-\int_{x-t}^x m(y)\mathrm{d}y}\mathrm{d}x.$$

and by using expression (28) and using the definition (22) of ω we obtain:

$$\begin{aligned}\left\|T_{(A+B)_{\overline{D(A)}}}(t)\begin{pmatrix}0\\ \phi\end{pmatrix}\right\|_X &= \frac{1}{\omega(0)}e^{-t\frac{\sigma}{f(L^\star)}}\int_0^\infty \omega(x+t)\frac{g(\chi^{-1}(x))}{g(\chi^{-1}(x+t))}\,|\phi(x)|\,\mathrm{d}x\\ &= \frac{1}{\omega(0)}e^{-t\frac{\sigma}{f(L^\star)}}\int_0^\infty \left(g(\chi^{-1}(x))+l(\chi^{-1}(x+t))g(\chi^{-1}(x))\right)|\phi(x)|\,\mathrm{d}x\,.\end{aligned}$$

Let us now find an estimate for the integrand, considering separately $[0,x_1]$ and $[x_1,+\infty)$, where x_1 will be precised later on. In what follows, we denote by c all the constants (that do not depend on x or t) that may change from line to line.

One can note that from the definition of χ and the mean value inequality we have that $\chi^{-1}(x+t)-\chi^{-1}(x)\le t\bar{g}$ where $\bar{g}:=\max\limits_{x\ge 0} g(x)$, and as l is increasing:

$$l(\chi^{-1}(x+t))\le l(\chi^{-1}(x)+t\bar{g})\,.$$

For $x\in[0,x_1]$, from assumptions (H2)-(H4), for all $\lambda>0$,

$$\begin{aligned}g(\chi^{-1}(x))+l(\chi^{-1}(x+t))g(\chi^{-1}(x)) &\le c+cl(\chi^{-1}(x)+t\bar{g})\\ &\le c+ce^{\lambda(\chi^{-1}(x)+t\bar{g})}\le ce^{\lambda\bar{g}t}.\end{aligned}$$

We choose λ such that $0<\lambda<\frac{\sigma}{2f(L^\star)\bar{g}}$ and, as $\omega(x)\ge\min\omega>0$ on $[0,x_1]$, we have

$$g(\chi^{-1}(x))+l(\chi^{-1}(x+t))g(\chi^{-1}(x))\le c\frac{\omega(x)}{\omega(x)}e^{\frac{\sigma}{2f(L^\star)}t}\le c\omega(x)e^{\frac{\sigma}{2f(L^\star)}t}\,.$$

For $x\ge x_1=\chi(x_0)$ and $t>\frac{x_0}{\bar{g}}$, with (H3) and (H2)-(H4):

$$l(\chi^{-1}(x+t))\le l(\chi^{-1}(x)+t\bar{g})\le cl(\chi^{-1}(x))l(t\bar{g})\le cl(\chi^{-1}(x))e^{t\frac{\sigma}{2f(L^\star)}}\,,$$

so, we have in the end the same bound as before, using expression (22) for ω,

$$g(\chi^{-1}(x)) + l(\chi^{-1}(x+t))g(\chi^{-1}(x)) \leq c\omega(x)e^{\frac{\sigma}{2f(L^\star)}t}\,.$$

So,

$$e^{-t\frac{\sigma}{f(L^\star)}}\frac{1}{\omega(0)}\int_0^\infty \left(g(\chi^{-1}(x)) + l(\chi^{-1}(x+t))g(\chi^{-1}(x))\right)|\phi(x)|\,\mathrm{d}x \leq ce^{-t\frac{\sigma}{2f(L^\star)}}\frac{1}{\omega(0)}\int_0^\infty \omega(x)\,|\phi(x)|\,\mathrm{d}x\,.$$

So finally, for t big enough (namely $t > \frac{x_0}{\bar{g}}$) :

$$\left\|T_{(A+B)_{\overline{D(A)}}}(t)\begin{pmatrix}0\\ \phi\end{pmatrix}\right\|_X \leq ce^{-t\frac{\sigma}{2f(L^\star)}}\left\|\begin{pmatrix}0\\ \phi\end{pmatrix}\right\|_X\,.$$

Therefore the growth bound of $(A+B)_{\overline{D(A)}}$ is negative, and, as a consequence, the essential growth bound of $(A + DG(\mathbf{w}^\star))_{\overline{D(A)}}$ is negative to. □

As the maximum between the spectral bound of $(A + DG(\mathbf{w}^\star))_{\overline{D(A)}}$ and its essential growth bound is equal to the maximum of the growth bound of its associated semigroup (corollary IV.2.11 in [8]), we can study the asymptotic of the linearized problem by studying the spectral bound of $(A + DG(\mathbf{w}^\star))_{\overline{D(A)}}$.

Proposition 6.

$$\sigma(A + DG(\mathbf{w}^\star)) \cap \left\{\lambda \in \mathbb{C} : \Re(\lambda) > -\frac{\sigma}{f(L^\star)}\right\} = \left\{\lambda \in \mathbb{C} : \Re(\lambda) > -\frac{\sigma}{f(L^\star)} \text{ and } \Delta(\lambda) = 0\right\}$$

with

$$\Delta(\lambda) = 1 - \frac{\rho f'(L^\star)}{f^2(L^\star)}\int_0^\infty l\circ\chi^{-1}(x)\exp\left(-\left(\frac{\sigma}{f(L^\star)}+\lambda\right)x\right)\mathrm{d}x$$
$$+\frac{\rho\sigma f'(L^\star)}{f^3(L^\star)}\int_0^\infty l\circ\chi^{-1}(x)\exp\left(-\frac{\sigma}{f(L^\star)}x\right)\frac{1}{\lambda}\left(1-e^{-\lambda x}\right)\mathrm{d}x.$$

Proof. First, for sake of readability, for all λ such that $\Re(\lambda) > -\frac{\sigma}{f(L^\star)}$, we define the function $\Theta \in \mathrm{L}^1([0,+\infty), \omega(x)\mathrm{d}x)$ as follows :

$$\Theta(x) = e^{-\int_0^x \lambda + m(\xi) + \frac{\sigma}{f(L^\star)}\mathrm{d}\xi}, \quad \forall x \in [0,+\infty)\,,$$

and the linear map $\mathcal{L} : \mathrm{L}^1([0,+\infty), \omega(x)\mathrm{d}x) \to \mathrm{L}^1([0,+\infty), \omega(x)\mathrm{d}x)$:

$$\mathcal{L}(\psi)(x) = \int_0^x \psi(\xi)e^{-\int_\xi^x(\lambda+m(\eta)+\frac{\sigma}{f(L^\star)})\mathrm{d}\eta}\mathrm{d}\xi, \quad \forall\psi \in \mathrm{L}^1([0,+\infty), \omega(x)\mathrm{d}x)\,, \forall x \in [0,+\infty)\,.$$

As

$$(\lambda I - (A+B)) \begin{pmatrix} 0 \\ \phi \end{pmatrix} = \begin{pmatrix} \phi(0) \\ \phi' + \left(\lambda + m(\cdot) + \frac{\sigma}{f(L^\star)}\right)\phi \end{pmatrix},$$

the resolvent operator $A+B$ is then given by, for $\lambda \in \mathbb{C}$, $\Re(\lambda) > -\frac{\sigma}{f(L^\star)}$ (similar calculation as in the proof of Prop 4)

$$(\lambda I - (A+B))^{-1} \begin{pmatrix} a \\ \psi \end{pmatrix} = \begin{pmatrix} 0 \\ a\Theta(x) + \mathcal{L}(\psi) \end{pmatrix}.$$

When $(\lambda I - (A+B))$ is invertible, $(\lambda I - (A+B+C))$ is invertible if and only if $I - C(\lambda I - (A+B))^{-1}$ is invertible, and we have:

$$(\lambda I - (A+B+C))^{-1} = (\lambda I - (A+B))^{-1}\left[I - C(\lambda I - (A+B))^{-1}\right]^{-1},$$

and by (26), we have :

$$I - C\left(\lambda I - (A+B)\right)^{-1} \begin{pmatrix} a \\ \psi \end{pmatrix} = \begin{pmatrix} a \\ \psi \end{pmatrix} - P\left(a\Theta(x) + \mathcal{L}(\psi)\right) \begin{pmatrix} c_1 \\ -c_2 w^* \end{pmatrix}$$

with P defined in Eq. (27), $c_1 = \frac{\rho}{g(r_{min})}\frac{f'(L^\star)}{f(L^\star)^2}$ and $c_2 = \sigma\frac{f'(L^\star)}{f(L^\star)^2}$.
Then,

$$\begin{aligned} & I - C\left(\lambda I - (A+B)\right)^{-1} \begin{pmatrix} a \\ \psi \end{pmatrix} = \begin{pmatrix} \hat{a} \\ \hat{\psi} \end{pmatrix} \\ \Leftrightarrow & \begin{cases} \hat{a} = a - c_1 P(a\Theta + \mathcal{L}(\psi)), \\ \hat{\psi} = \psi + c_2 P(a\Theta + \mathcal{L}(\psi)) w^\star. \end{cases} \end{aligned} \tag{29}$$

By applying $P \circ \mathcal{L}$ to the second equation, and by linearity, we obtain

$$\begin{cases} \hat{a} = a\left(1 - c_1 P(\Theta)\right) - c_1 P(\mathcal{L}(\psi)), \\ P(\mathcal{L}(\hat{\psi})) = P(\mathcal{L}(\psi))\left(1 + c_2 P(\mathcal{L}(w^\star))\right) + a c_2 P(\Theta) P(\mathcal{L}(w^\star)). \end{cases}$$

This linear system can be written as

$$\begin{pmatrix} 1 - c_1 P(\Theta) & -c_1 \\ c_2 P(\Theta) P(\mathcal{L}(w^\star)) & 1 + c_2 P(\mathcal{L}(w^\star)) \end{pmatrix} \begin{pmatrix} a \\ P(\mathcal{L}(\psi)) \end{pmatrix} = \begin{pmatrix} \hat{a} \\ P(\mathcal{L}(\hat{\psi})) \end{pmatrix}.$$

The determinant of the matrix is given by:

$$\Delta(\lambda) := (1 - c_1 P(\Theta))(1 + c_2 P(\mathcal{L}(w^\star))) + c_1 c_2 P(\Theta) P(\mathcal{L}(w^\star)) = 1 - c_1 P(\Theta) + c_2 P(\mathcal{L}(w^\star)).$$

Therefore, if $\Delta(\lambda) \neq 0$, then $I - C(\lambda I - (A+B))^{-1}$ is invertible, so $(\lambda I - (A+B+C))$ is invertible too, which implies that:

$$\left\{\lambda \in \mathbb{C} : \Re(\lambda) > -\frac{\sigma}{f(L^\star)} \text{ and } \Delta(\lambda) \neq 0\right\} \subset \rho\left(\lambda I - (A+B+C)\right) \cap \left\{\lambda \in \mathbb{C} : \Re(\lambda) > -\frac{\sigma}{f(L^\star)}\right\}$$

such that

$$\sigma\left(\lambda I - (A+B+C)\right) \cap \left\{\lambda \in \mathbb{C} : \Re(\lambda) > -\frac{\sigma}{f(L^\star)}\right\} \subset \left\{\lambda \in \mathbb{C} : \Re(\lambda) > -\frac{\sigma}{f(L^\star)} \text{ and } \Delta(\lambda) = 0\right\}.$$

On the other hand, if $\Delta(\lambda) = 0$ let us show that we can find $\begin{pmatrix} a \\ \psi \end{pmatrix} \in X \setminus \{0\}$ such that $I - C(\lambda I - (A+B))^{-1} \begin{pmatrix} a \\ \psi \end{pmatrix} = 0$, which is equivalent to find $\begin{pmatrix} 0 \\ \phi \end{pmatrix} \in D(A) \setminus \{0\}$ in the kernel of $\lambda I - (A+B+C)$.
Indeed, we set $a \neq 0$ and $\psi := -ac_2 P(\Theta) w^\star + \frac{ac_2^2}{c_1} P(\mathcal{L}(w^\star)) w^\star$. Then, as $\Delta(\lambda) = 0$,

$$P(\mathcal{L}(\psi)) = -ac_2 P(\Theta) P(\mathcal{L}(w^\star)) + \frac{ac_2^2}{c_1} P(\mathcal{L}(w^\star))^2 = \frac{ac_2}{c_1} P(\mathcal{L}(w^\star)) \left(\Delta(\lambda) - 1\right) = -\frac{ac_2}{c_1} P(\mathcal{L}(w^\star)),$$

so

$$\begin{aligned} \psi + c_2 P(a\Theta + \mathcal{L}(\psi)) w^\star &= \frac{ac_2^2}{c_1} P(\mathcal{L}(w^\star)) w^\star + c_2 P(\mathcal{L}(\psi)) w^\star \\ &= \frac{ac_2^2}{c_1} P(\mathcal{L}(w^\star)) w^\star - \frac{ac_2^2}{c_1} P(\mathcal{L}(w^\star)) w^\star = 0. \end{aligned}$$

Furthermore,

$$a - c_1 P(a\Theta + \mathcal{L}(\psi)) = a - ac_1 P(\Theta) + ac_2 P(\mathcal{L}(w^\star)) = a\Delta(\lambda) = 0.$$

Hence, from (29), $I - C(\lambda I - (A+B))^{-1} \begin{pmatrix} a \\ \psi \end{pmatrix} = 0$, thus

$$\left\{\lambda \in \mathbb{C} : \Re(\lambda) > -\frac{\sigma}{f(L^\star)} \text{ and } \Delta(\lambda) = 0\right\} \subset \sigma\left(\lambda I - (A+B+C)\right) \cap \left\{\lambda \in \mathbb{C} : \Re(\lambda) > -\frac{\sigma}{f(L^\star)}\right\}.$$

To end with this proof, we simplify the expression of Δ (with expression (28), using the formula (8) for $w^\star = u^\star \circ \chi^{-1}$ and a change of variables):

$$\begin{aligned} \Delta(\lambda) = 1 &- \frac{f'(L^\star)}{f^2(L^\star)} \int_{r_{min}}^{\infty} q(x) \exp\left(-\left(\frac{\sigma}{f(L^\star)} + \lambda\right) \chi(x)\right) \mathrm{d}x \\ &+ \frac{\sigma f'(L^\star)}{f^3(L^\star)} \int_{r_{min}}^{\infty} q(x) \exp\left(-\frac{\sigma}{f(L^\star)} \chi(x)\right) \left(\int_{r_{min}}^{x} \frac{1}{g(y)} \exp\left(-\lambda \int_y^x \frac{1}{g(z)} \mathrm{d}z\right) \mathrm{d}y\right) \mathrm{d}x, \end{aligned}$$

where $q(x) := \rho \dfrac{l(x)}{g(x)}$ and $\chi(x) := \displaystyle\int_{r_{min}}^{x} \frac{1}{g(s)} \mathrm{d}s$. With a change of variables in the integral within the second integral term, we can verify that:

$$\Delta(\lambda) = 1 - \frac{f'(L^\star)}{f^2(L^\star)} \int_{r_{min}}^{\infty} q(x) \exp\left(- \left(\frac{\sigma}{f(L^\star)} + \lambda \right) \chi(x) \right) \mathrm{d}x$$
$$+ \frac{\sigma f'(L^\star)}{f^3(L^\star)} \int_{r_{min}}^{\infty} q(x) \exp\left(- \frac{\sigma}{f(L^\star)} \chi(x) \right) \left(\int_0^{\chi(x)} e^{-\lambda y} \mathrm{d}y \right) \mathrm{d}x,$$

and with the change of variable $z = \chi(x)$,recalling that p is defined at Eq.(17) by $p(x) = l \circ \chi^{-1}(x)$,

$$\begin{aligned}
\Delta(\lambda) &= 1 - \frac{\rho f'(L^\star)}{f^2(L^\star)} \int_0^{\infty} p(z) \exp\left(- \left(\frac{\sigma}{f(L^\star)} + \lambda \right) z \right) \mathrm{d}z \\
&+ \frac{\rho \sigma f'(L^\star)}{f^3(L^\star)} \int_0^{\infty} p(z) \exp\left(- \frac{\sigma}{f(L^\star)} z \right) \left(\int_0^{z} e^{-\lambda y} \mathrm{d}y \right) \mathrm{d}z \\
&= 1 - \frac{\rho f'(L^\star)}{f^2(L^\star)} \int_0^{\infty} p(z) \exp\left(- \left(\frac{\sigma}{f(L^\star)} + \lambda \right) z \right) \mathrm{d}z \\
&+ \frac{\rho \sigma f'(L^\star)}{f^3(L^\star)} \int_0^{\infty} p(z) \exp\left(- \frac{\sigma}{f(L^\star)} z \right) \frac{1}{\lambda} \left(1 - e^{-\lambda z} \right) \mathrm{d}z.
\end{aligned}$$

□

B Figures

On Figure 6, we show the evolution of solution to system (1)- (2)-(4) with respect to time. The numerical simulation presented here is performed in two steps : first a numerical resolution of PDE (1) is computed with a standard Euler explicit in time and upwind finite volume scheme in space and, in a second step, the extracellular lipid amount is updated with the new density thanks to Eq.(4). The upwind finite volume scheme is particularly easy to implement here since the velocity is always positive.

We start from an initial cell size distribution, where all the cells are empty and therefore the whole quantity of lipids $L_0 = 10$ nmol is outside cells. At early times, the lipids enter cells progressively, see the top left panel, until nearly no extracellular lipids are left. More precisely, at early times, radii are increasing and radius of 11μm is reached at $t = 100$, 13μm at $t = 200$, 15μm at $t = 300$ and 17μm at $t = 300$, see on bottom left panel. Then, at around $t = 900$, a peak of adipocytes with a very small radius appears and those cells are growing until the stationary distribution is reached, see on bottom right panel. We notice that the extracellular

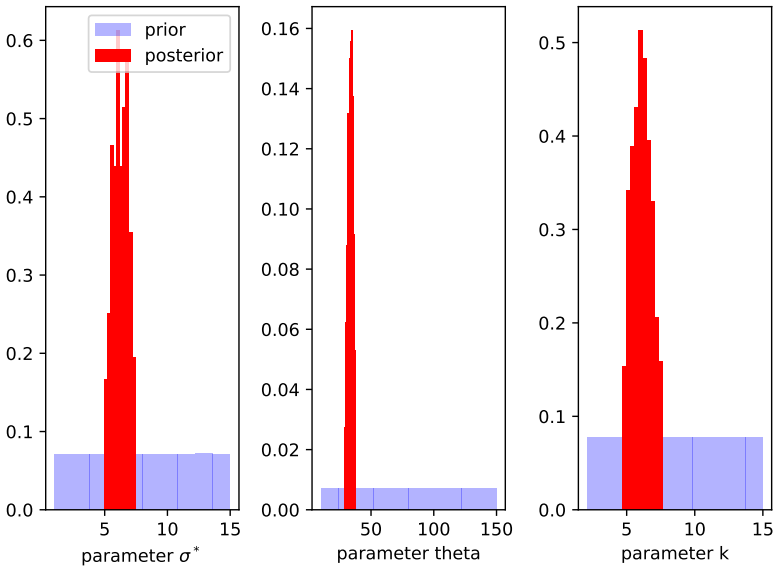

Figure 5: Prior and posterior parameter distributions from ABC rejection sampler algorithm. The posterior parameter distributions are obtained with cell size distribution of rat 1. The procedure was repeated 10^6 times and the threshold was set to $5\,10^{-4}$.

quantity of lipids is oscillating before reaching the stationary value, see on top right panel. This is coherent with the analytical result of the article since the eigenvalues of the linearized system are complex with a strictly negative real part, which leads to oscillating behavior of the system.

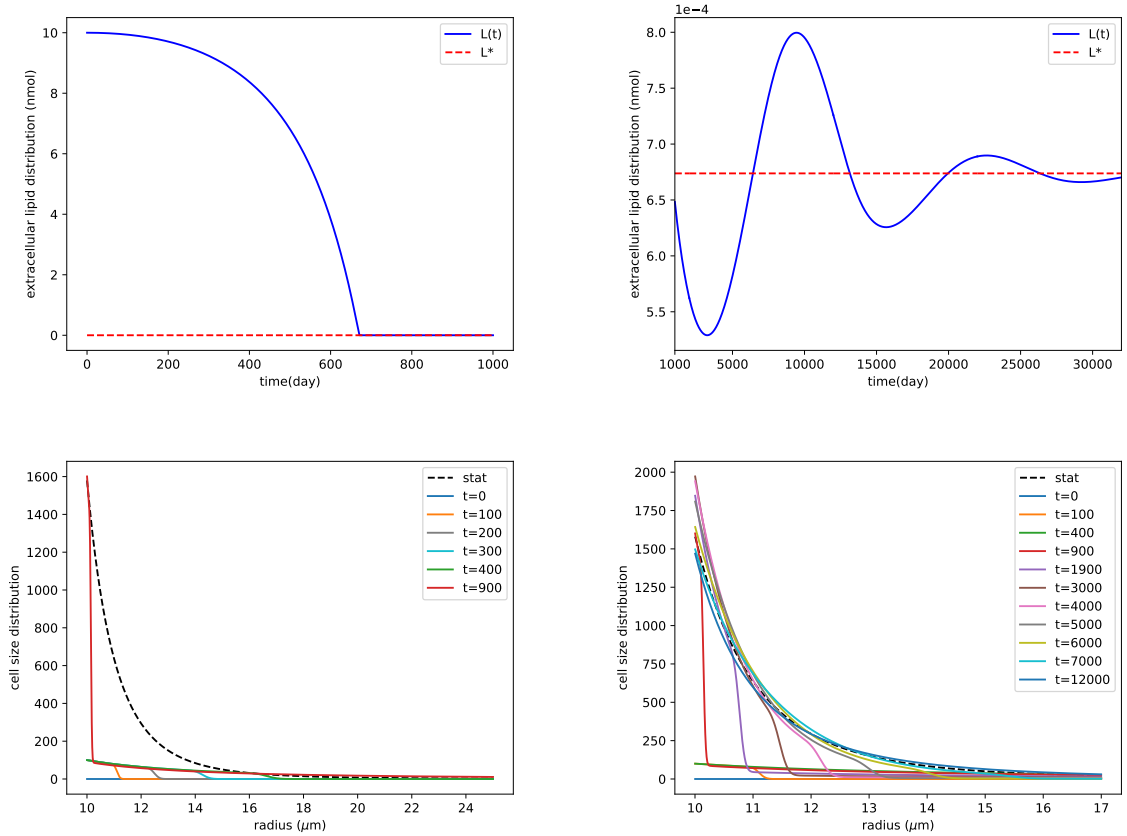

Figure 6: Time evolution of solutions to system (1)- (2)-(4). Top left : evolution of the extracellular lipid quantity with respect to time for early times ($0 \leq t \leq 1000$) Top right: evolution of the extracellular lipid quantity with respect to time for large times ($1000 \leq t \leq 32000$) Bottom left: cell size distribution with respect to radius for different early times ($0 \leq t \leq 900$). Only the left part of the distribution is displayed (radius between $10\mu m$ and $25\mu m$). Bottom right : cell size distribution with respect to radius for several times ($0 \leq t \leq 12000$). Only the left part of the distribution is displayed (radius between $10\mu m$ and $17\mu m$). Parameters are: $k = 6$, $\theta = 50\mu$m, $\alpha = 10^{-4}\mu\text{m}^{-1}.\text{time}^{-1}$, $\sigma = 5.10^{-4}$ time^{-1}, $r_{min} = 10\mu$m.

References

[1] Tomás Cabeza De Baca, Shannon Parrington, Susanne Votruba, Paolo Piaggi, Jonathan Krakoff, and Douglas C. Chang. Adipocyte size, adipose tissue calories, and circulating adipokines, before and after diet-induced weight loss in humans. *Endocrine*, 84(2):490–499, 2024.

[2] Juan Calvo, Erwan Hingant, and Romain Yvinec. The initial-boundary value problem for the Lifshitz–Slyozov equation with non-smooth rates at the boundary. *Nonlinearity*, 34(4):1975–2017, February 2021.

[3] S. Cinti, G. Mitchell, G. Barbatelli, I. Murano, E. Ceresi, E. Faloia, S. Wang, M. Fortier, A.S. Greenberg, and M.S. Obin. Adipocyte death defines macrophage localization and function in adipose tissue of obese mice and humans. *J Lipid Res.*, 46(11):2347–55, 2005.

[4] Frédérique Clément, Louis Fostier, and Romain Yvinec. Well-posedness and bifurcation analysis of a size-structured population model: Application to female gametes dynamics. September 2024.

[5] Jean-François Collet and Thierry Goudon. On solutions of the Lifshitz-Slyozov model. *Nonlinearity*, 13(4):1239, 2000.

[6] Aloïs Dauger, Hedi Soula, and Chloe Audebert. Adipocyte size distribution: Mathematical model of a tissue property. *Mathematical Biosciences*, 384:109433, 2025.

[7] A. Ducrot, Z. Liu, and P. Magal. Essential growth rate for bounded linear perturbation of non-densely defined Cauchy problems. *J. Math. Anal. Appl.*, 341(1):501–518, May 2008.

[8] Klaus-Jochen Engel and Rainer Nagel. *One-Parameter Semigroups for Linear Evolution Equations*. Springer-Verlag New York, 2000.

[9] Anne-Sophie Giacobbi, Leo Meyer, Magali Ribot, Romain Yvinec, Hedi Soula, and Chloe Audebert. Mathematical modeling of adipocyte size distributions: Identifiability and parameter estimation from rat data. *Journal of Theoretical Biology*, 581:111747, March 2024.

[10] A. Grabosch and H. J. A. M. Heijmans. Cauchy problems with state-dependent time evolution. *Japan J. Appl. Math.*, 7(3):433–457, October 1990.

[11] Annette Grabosch and Henk J. A. M. Heijmans. Production, development, and maturation of red blood cells. In Ovide Arino, David E. Axelrod, and Marek Kimmel, editors, *Mathematical population dynamics*, pages 189–210. CRC Press, 1991.

[12] Sang Mun Han, Hahn Nahmgoong, Kyung Min Yim, and Jae Bum Kim. How obesity affects adipocyte turnover. *Trends in Endocrinology & Metabolism*, 36(2):147–160, 2025.

[13] F. Mólgaard Hansen, J. Høiriis Nielsen, and J. Gliemann. The influence of body weight and cell size on lipogenesis and lipolysis of isolated rat fat cells*. *European Journal of Clinical Investigation*, 4(1):411–418, February 1974.

[14] Gliemann J and Vinten J. Lipogenesis and insulin sensitivity of single fat cells. *J Physiol*, 236(3):499–516, 1974.

[15] M. Jacquier, F. Crauste, C.O. Soulage, and H.A. Soula. A predictive model of the dynamics of body weight and food intake in rats submitted to caloric restrictions. *PLOS ONE*, 9(6):e100073, 2014.

[16] J. Jo, J. Guo, T. Liu, S. Mullen, K.D. Hall, S.W. Cushman, and V. Periwal. Hypertrophy-driven adipocyte death overwhelms recruitment under prolonged weight gain. *Biophys J.*, 99(11):3535–44, 2010.

[17] Junghyo Jo, Oksana Gavrilova, Stephanie Pack, William Jou, Shawn Mullen, Anne E. Sumner, Samuel W. Cushman, and Vipul Periwal. Hypertrophy and/or hyperplasia: Dynamics of adipose tissue growth. *PLoS Computational Biology*, 5(3):e1000324, March 2009.

[18] Junghyo Jo, Zeina Shreif, and Vipul Periwal. Quantitative dynamics of adipose cells. *Adipocyte*, 1:80–88, 2012.

[19] Soo M Kim, Mingyue Lun, Mei Wang, Samuel E Senyo, Christelle Guillermier, Parth Patwari, and Matthew L Steinhauser. Loss of white adipose hyperplastic potential is associated with enhanced susceptibility to insulin resistance. *Cell Metab.*, 20(6):1049–1058, December 2014.

[20] Max Lafontan and Michel Berlan. Fat cell $\alpha 2$ -adrenoceptors: The regulation of fat cell function and lipolysis*. *Endocrine Reviews*, 16(6):716–738, December 1995.

[21] Philippe Laurençot. Weak Solutions to the Lifshitz-Slyozov-Wagner Equation. *Indiana University mathematics journal*, 50(3):1319–1346, 2001.

[22] Soazig Le Lay, Stéphane Krief, Céline Farnier, Isabelle Lefrère, Xavier Le Liepvre, Raymond Bazin, Pascal Ferré, and Isabelle Dugail. Cholesterol, a cell size-dependent signal that regulates glucose metabolism and gene expression in adipocytes. *Journal of Biological Chemistry*, 276(20):16904–16910, May 2001.

[23] Yizhe Lim and Joshua Boster. *Obesity and Comorbid Conditions*. StatPearls Publishing, Treasure Island (FL), 2025.

[24] Alice Liu, Alper Sonmez, Gail Yee, Merlijn Bazuine, Matilde Arroyo, Arthur Sherman, Tracey McLaughlin, Gerald Reaven, Samuel Cushman, and Philip Tsao. Differential adipogenic and inflammatory properties of small adipocytes in zucker obese and lean rats. *Diabetes and Vascular Disease Research*, 7(4):311–318, October 2010.

[25] Jennifer MacKellar, Samuel W. Cushman, and Vipul Periwal. Waves of adipose tissue growth in the genetically obese zucker fatty rat. *PLoS ONE*, 5, 2010.

[26] Pierre Magal and Shigui Ruan. *Theory and applications of abstract semilinear Cauchy problems*, volume 201 of *Appl. Math. Sci.* Springer International Publishing, 2018.

[27] T. McLaughlin, A. Sherman, P. Tsao, O. Gonzalez, G. Yee, C. Lamendola, G. M. Reaven, and S. W. Cushman. Enhanced proportion of small adipose cells in insulin-resistant vs insulin-sensitive obese individuals implicates impaired adipogenesis. *Diabetologia*, 50(8):1707–1715, July 2007.

[28] Léo Meyer, Magali Ribot, and Romain Yvinec. A lifshitz–slyozov type model for adipocyte size dynamics: limit from becker–döring system and numerical simulation. *Journal of Mathematical Biology*, 88(2):16, February 2024.

[29] R. A. Neese, L. M. Misell, S. Turner, A. Chu, J. Kim, D. Cesar, R. Hoh, F. Antelo, A. Strawford, J. M. McCune, M. Christiansen, and M. K. Hellerstein. Measurement in vivo of proliferation rates of slow turnover cells by 2h2o labeling of the deoxyribose moiety of dna. *Proceedings of the National Academy of Sciences*, 99(24):15345–15350, November 2002.

[30] Alessandra Rigamonti, Kristen Brennand, Frank Lau, and Chad A Cowan. Rapid cellular turnover in adipose tissue. *PLoS One*, 6(3):e17637, March 2011.

[31] Alexander Sakers, Mirian Krystel De Siqueira, Patrick Seale, and Claudio J. Villanueva. Adipose-tissue plasticity in health and disease. *Cell*, 185:419–446, 2 2022.

[32] Nicola Santoro, Romy Kursawe, Ebe D'Adamo, Daniel J. Dykas, Clarence K. Zhang, Allen E. Bale, Anna M. Calí, Deepak Narayan, Melissa M. Shaw, Bridget Pierpont, Mary Savoye, Derek Lartaud, Samuel Eldrich, Samuel W. Cushman, Hongyu Zhao, Gerald I. Shulman, and Sonia Caprio. A common variant in the patatin-like phospholipase 3 gene (pnpla3) is associated with fatty liver disease in obese children and adolescents. *Hepatology*, 52(4):1281–1290, October 2010.

[33] Thomas Skurk, Catherine Alberti-Huber, Christian Herder, and Hans Hauner. Relationship between adipocyte size and adipokine expression and secretion. *The Journal of Clinical Endocrinology & Metabolism*, 92(3):1023–1033, March 2007.

[34] Ulf Smith. Effect of cell size on lipid synthesis by human adipose tissue in vitro. *Journal of Lipid Research*, 12(1):65–70, 1971.

[35] H.A. Soula, A. Géloën, and C.O. Soulage. Model of adipose tissue cellularity dynamics during food restriction. *Journal of Theoretical Biology*, 364:189–196, January 2015.

[36] H.A. Soula, H. Julienne, C.O. Soulage, and A. Géloën. Modelling adipocytes size distribution. *Journal of Theoretical Biology*, 332:89–95, September 2013.

[37] Kirsty L. Spalding, Erik Arner, Pål O. Westermark, Samuel Bernard, Bruce A. Buchholz, Olaf Bergmann, Lennart Blomqvist, Johan Hoffstedt, Erik Näslund, Tom Britton, Hernan Concha, Moustapha Hassan, Mikael Rydén, Jonas Frisén, and Peter Arner. Dynamics of fat cell turnover in humans. *Nature*, 453(7196):783–787, June 2008.

[38] Tina Toni, David Welch, Natalja Strelkowa, Andreas Ipsen, and Michael P.H. Stumpf. Approximate bayesian computation scheme for parameter inference and model selection in dynamical systems. *Journal of the Royal Society Interface*, 6:187–202, 2009.

[39] Paul Trayhurn. Hypoxia and adipose tissue function and dysfunction in obesity. *Physiological Reviews*, 93(1):1–21, January 2013.

[40] L. Turner, M.-F. Gauthier, A. Lafortune, A. Tchernof, and S. Santosa. Adipocyte size, adipose tissue fibrosis, macrophage infiltration and disease risk are different in younger and older individuals with childhood versus adulthood onset obesity. *International Journal of Obesity*, 46(10):1859–1866, October 2022.

[41] Yi Ching Esther Wan, Jeremy Dufau, and Kirsty L. Spalding. Local and systemic impact of adipocyte senescence-associated secretory profile. *Current Opinion in Endocrine and Metabolic Research*, 37:100547, December 2024.